

Supporting Information for

Power characteristics of spinel cathode correlated
with elastic softness and phase transformation for
high-power lithium-ion batteries

Jin-Myoung Lim,^{a,†} Rye-Gyeong Oh,^{b,†} Woosuk Cho,^b Kyeongjae Cho,^{,c} Maenghyo Cho,^{*,a} and
Min-Sik Park^{*,d}*

^a Department of Mechanical and Aerospace Engineering, Seoul National University, 1 Gwanak-ro, Gwanak-gu, Seoul 08826, the Republic of Korea

^b Advanced Batteries Research Center, Korea Electronics Technology Institute, 25 Saenari-ro, Bundang-gu, Seongnam 13509, the Republic of Korea

^c Department of Materials Science and Engineering and Department of Physics, University of Texas at Dallas, Richardson, TX 75080, USA

^d Department of Advanced Materials Engineering for Information and Electronics, Kyung Hee University, 1732 Deogyeong-daero, Gi-heung-gu, Yongin 17104, the Republic of Korea

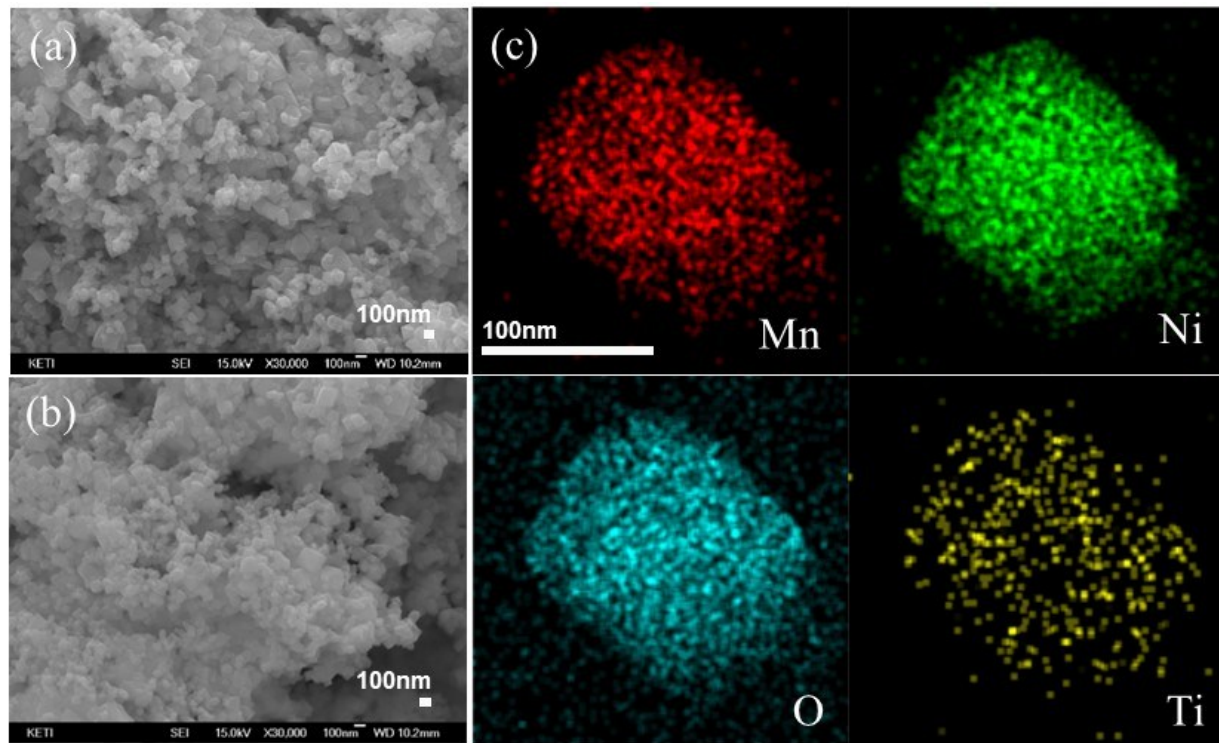


Fig. S1. (a, b) FESEM images of (a) LNMO and (b) LNMTO nanopowders, and (c) EDS mapping images of ion-sliced HRTEM for Mn, Ni, O, and Ti ions in a LNMTO nanoparticle.

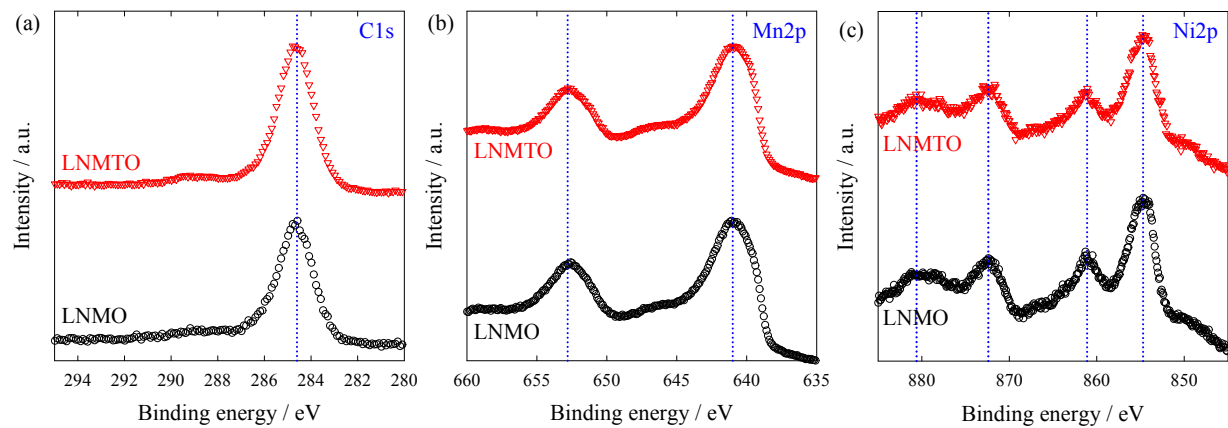


Fig. S2. XPS spectra of (a) C1s, (b) Mn2p, and (c) Ni2p for LNMO (black circles) and LNMTO (red triangles) after Ar ion sputtering for 300 s.

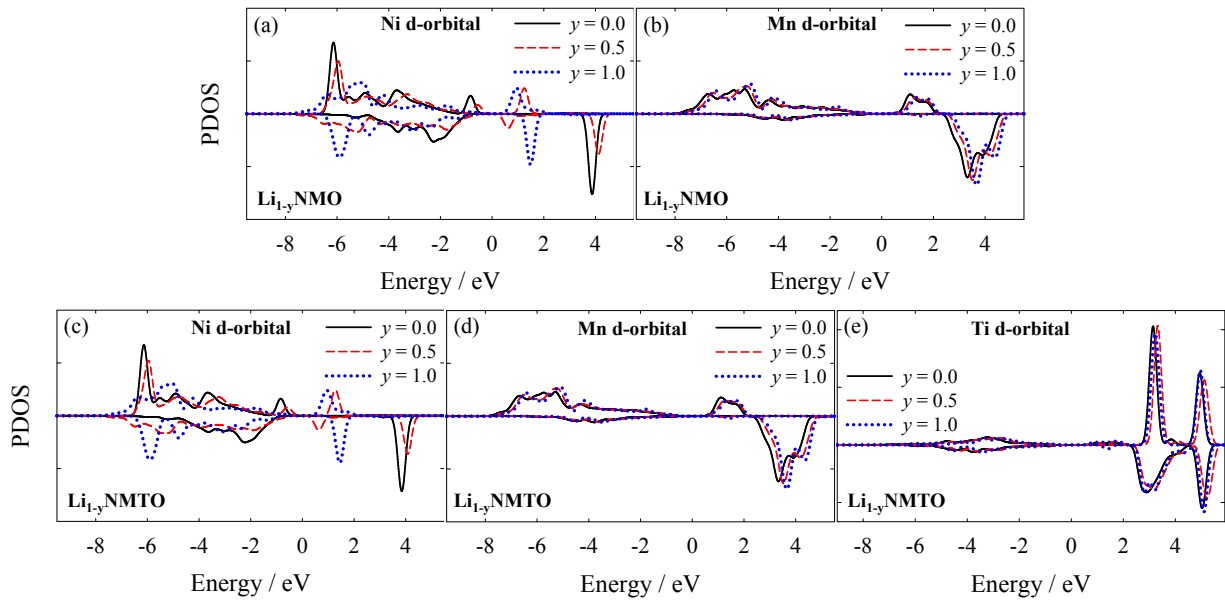


Fig. S3. PDOS of (a) Ni and (b) Mn d-orbitals in L_{1-y}NMO , and (c) Ni, (d) Mn, and (e) Ti d-orbitals in $\text{L}_{1-y}\text{NMTO}$ with respect to the inverse Li content, $y = 0$ (black solid line), 0.5 (red dashed line), and 1.0 (blue dotted line).

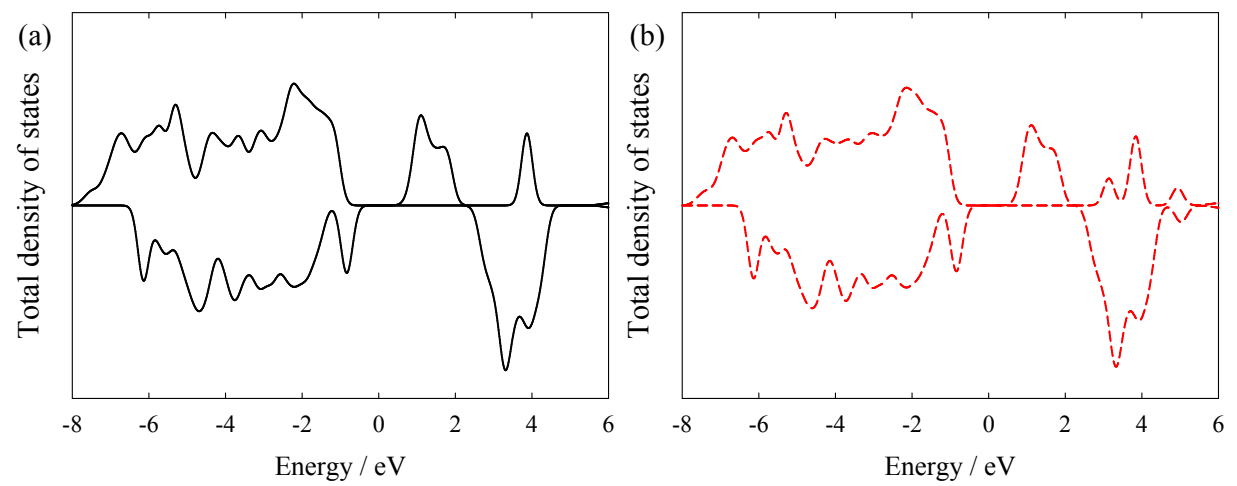


Fig. S4. Total density of states of (a) LNMO (black solid line) and (b) LNMTO (red dashed line).

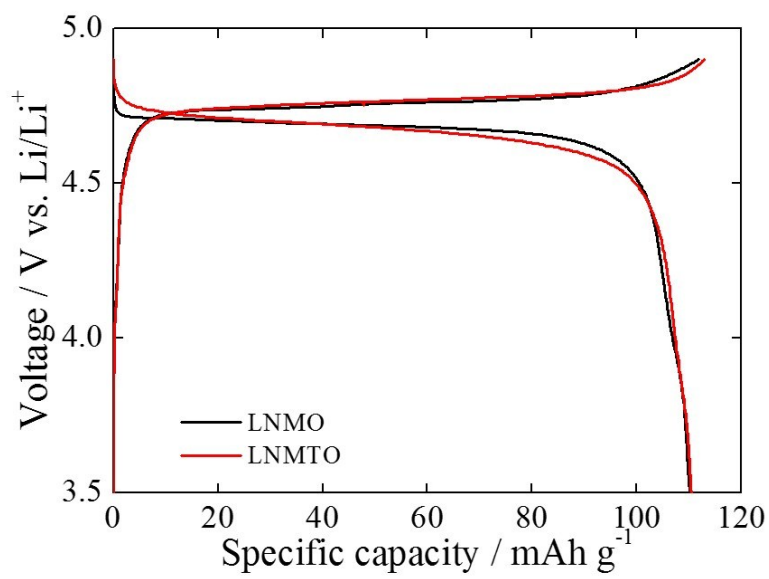


Fig. S5. Charge-discharge profiles of LNMO (black lines) and LNMTO (red lines) at a specific current of 80 mA g⁻¹.